Thermodynamic Assessment of the Stability of Thrombin Receptor Antagonistic Peptides in Hydrophobic Environments

Reinhard I. Boysen, Agnes J. O. Jong, and Milton T. W. Hearn
Centre for Bioprocess Technology, Department of Biochemistry and Molecular Biology, Monash University, Victoria 3800, Australia

ABSTRACT In this paper, a general procedure is described to determine thermodynamic parameters associated with the interaction of thrombin receptor antagonistic peptides (TRAPs) with immobilized nonpolar ligands. The results show that these interactions were associated with nonlinear van't Hoff dependencies over a wide temperature range. Moreover, changes in relevant thermodynamic parameters, namely the changes in Gibbs free energy of interaction, ΔG^0_{assoc}, enthalpy of interaction, ΔH^0_{assoc}, entropy of interaction, ΔS^0_{assoc}, and heat capacity, ΔC^0_p, have been related to the structural properties of these TRAP analogs. The implications of these investigations for the design of thrombin receptor agonists/antagonists with structures stabilized by intramolecular hydrophobic interactions are discussed.

LIST OF SYMBOLS

$b_{(0)}$, $b_{(1)}$, $b_{(2)}$, $b_{(3)}$ . . .	Coefficients for the polynomial dependency of ln k' versus $1/T$
c_1	Mole fraction of displacing solvent
ΔA_{apolar}	Apolar accessible surface area
ΔA_{polar}	Polar accessible surface area
ΔA_{total}	Total accessible surface area
ΔC^0_p	Change in the heat capacity for the association of the polypeptide P_i with the nonpolar ligands
ΔG^0_{assoc}	Change in Gibbs free energy due to the association of the polypeptide P_i with the nonpolar ligands
ΔH^0_{assoc}	Change in the enthalpy due to the association of the polypeptide P_i with the nonpolar ligands
ΔS^0_{assoc}	Change in the entropy due to the association of the polypeptide P_i with the nonpolar ligands
φ	Volume fraction of organic solvent in binary water–solvent mixture
Φ	Phase ratio of the chromatographic system ($= V_S/V_M$)
K_{assoc}	Equilibrium binding constant
k'	Capacity factor, $k' = (t_e - t_0)/t_0 = (n_S/n_M) \times (V_S/V_M) = K_{assoc} \times \Phi$
ln k'	Logarithm of the capacity factor, k'
ln k_0	Value of ln k' when $c_i \rightarrow 0$, or $\varphi \rightarrow 0$
n_S	Number of moles of the peptide in the bound states
n_M	Number of moles of the peptide in the free states
N_{res}	Number of amino acid residues in a polypeptide
r^2	Correlation coefficient
R	Gas constant
t_0	Retention time of noninteracting solute
t_e	Retention time of a polypeptide P_i
T	Temperature in degrees Kelvin
T_H	Temperature at which $\Delta H^0_{assoc} \rightarrow 0$
T_S	Temperature at which $T\Delta S^0_{assoc} \rightarrow 0$
V_M	Volume of the solvent in the system
V_S	Volume of the immobilized ligands plus support matrix in the system

INTRODUCTION

Protease-activated receptors (PARs) play an important role in platelet function. In particular, various serine proteases, including thrombin, are known to activate PARs by cleaving their amino-terminal extracellular domains to reveal a new amino terminus that can then function as a tethered ligand. By binding intramolecularly to the receptor, the tethered ligand causes transmembrane signaling (Vu et al., 1991). In human platelets, a dual receptor system for the activation of PARs has been found to occur (Kahn et al., 1998). From an experimental perspective, the existence of this second receptor-mediated pathway adds a further level of complexity in the cell biology of PAR activation. However, it also has the potential to provide exquisite levels of regulation for a diverse range of physiological functions, including a safeguard against irreversible activation or inhibition of a single class of PAR receptor by potent agonists/antagonists.

The thrombin receptor (PAR-1) is a transmembrane G-protein-coupled structure that is activated by serine protease cleavage of its extracellular N-terminus to expose an agonist peptide ligand that is tethered to the receptor itself. Synthetic peptides that contain the agonist motif of human PAR-1, such as H-Ser-Phe-Leu-Leu-Arg-Asn-Pro-OH (TRAP-1) (Mari et al., 1994), are capable of receptor activation in the absence of thrombin. TRAP-1 has been used as a pharmacological tool to probe the function of the PAR-1 receptor in various cell types (Mari et al., 1994; Seiler et al.,

Submitted February 13, 2001, and accepted for publication January 31, 2002.

Address reprint requests to Milton T. W. Hearn, Centre for Bioprocess Technology, Dept. of Biochemistry and Molecular Biology, Monash University, P.O. Box 13D, Victoria 3800, Australia. Fax: +61-3-9905-5882; E-mail: milton.hearn@med.monash.edu.au.

0006-3495/02/05/2279/14 $2.00

TABLE 1 Peptide code, sequence, molecular weight (MW), accessible surface areas, ΔA_{tot} (Å^2) for the unfolded and folded forms of the peptide analogs, relative hydrophobicity, and RP-HPLC elution order of the TRAP peptide analogs

Peptide	Sequence	MW	ΔA_{tot} (Å^2)*		Relative Hydrophobicity, χ_{hydr}†	RP-HPLC Elution Order‡
			Unfolded	Globular		
TRAP-1	Ser-Phe-Leu-Leu-Arg-Asn-Pro	846.0	1015.2	917.0	20.86	4
TRAP-2	Ser-**Ala**-Leu-Leu-Arg-Asn-Pro	769.9	923.9	855.9	14.24	1
TRAP-3	Ser-Phe-**Ala**-Leu-Arg-Asn-Pro	803.9	964.7	883.4	16.91	3
TRAP-4	Ser-Phe-Leu-**Ala**-Arg-Asn-Pro	803.9	964.7	883.4	16.91	2
TRAP-5	Ser-Phe-Leu-Leu-**Ala**-Asn-Pro	760.9	913.1	848.5	22.22	5
TRAP-6	Ser-Phe-Leu-Leu-Arg-**Ala**-Pro	803.3	964.0	882.9	24.75	6

*The accessible surface areas ΔA_{tot} (Å^2) for unfolded peptides were calculated according to the relationship $\Delta A_{tot} = 1.2$ (MW) (Spassov et al., 1997) and for globular peptides according to the relationship $\Delta A_{tot} = 6.6$ (MW)$^{0.732}$ (Makhatadze and Privalov, 1995), where MW is the molecular weight.
†The relative hydrophobicity of the TRAP peptide analogs in the presence of immobilized *n*-octyl ligands were calculated according Wilce et al. (1995).
‡The RP-HPLC elution order was determined under isocratic conditions on Zorbax 300SB-C8 columns using water-acetonitrile (86:14 v/v) containing 0.09% (v/v) TFA.

1996). Replacement of Phe^2 with Ala in TRAP-1, with elimination of the β-phenyl side chain group, results in complete receptor inactivation (Nose et al., 1998a). Other results indicated that the electrostatic interaction of the guanidino-group of Arg^5 is important for TRAP-1 to interact with its receptor (Nose et al., 1998b). On the basis of introduced conformational perturbations, structure–function relationships of various bioactive thrombin receptor-activating peptide analogs (TRAPs), prepared by solid phase peptide synthesis procedures, have been explored in vitro with cultured human glomerular messiangial cells (Troyer et al., 1992), naturally thrombin-responsive CCL-29 cells and Jurkat T cells (Mari et al., 1994) and in vivo in rabbit models (M. Cunningham, K. Tipping, S. Holdsworth, R. I. Boysen, and M. T. W. Hearn, unpublished results). Based on these latter and other studies (Ceruso et al., 1999), it has been proposed that an extended structure of the agonist peptide is responsible for receptor recognition, with a hydrophobic contact occurring between the side chains of Phe^2 and Leu^4.

To gain further insight into the conformational and interactive behavior of TRAP analogs, the interaction of TRAP-1 and a complete set of Ala-replacement analogs (Table 1) with immobilized *n*-octyl ligands has been investigated. The use of immobilized *n*-alkyl or phospholipid ligands to illuminate the biophysical basis of the structure–function behavior of bioactive peptides has attracted increasing attention during the past several years (Houston et al., 1998; Kondejewski et al., 1999; Beyermann et al., 1996; Hearn, 2001b). In particular, these procedures permit the thermodynamics of peptide–ligand interaction to be studied. Insight can thus be gained into the role of intramolecular hydrophobic stabilization or the consequences of solvation/desolvation effects, permitting correlations to be established with membrane-associated receptor binding events and the respective changes in the Gibbs free energy, ΔG^0_{assoc}, enthalpy, ΔH^0_{assoc}, entropy, ΔS^0_{assoc}, and heat capacity, ΔC^0_p, for peptide–ligand interactions determined. In the present studies, changes in thermodynamic parameters associated with TRAP-peptide–*n*-octyl ligand interactions have been evaluated in terms of the molecular structure and the associated linear free energy relationships of these peptides. Based on these results, guidelines can be proposed to facilitate the design of TRAP-1 analogs with enhanced stability in nonpolar environments.

EXPERIMENTAL PROCEDURES

Chemicals and reagents

Acetonitrile (HPLC grade) was obtained from Biolab Scientific Pty. Ltd. (Sydney, Australia); all other solvents were of analytical grade. Water was distilled and deionized in a Milli-Q system (Millipore, Bedford, MA). Trifluoroacetic acid (TFA), *N*,*N*-dimethylformamide (DMF), piperidine, 1-hydroxybenzotriazole (HOBt), O-benzotriazole-*N*,*N*,*N*′,*N*′-tetramethyl-uronium-hexafluorophosphate (HBTU), Boc-L-Pro-PAM-resin and all of the L-α-Boc-protected and L-α-Fmoc-protected amino acids were obtained from Auspep Pty. Ltd. (Melbourne, Australia). Thioanisole, acetic anhydride, 1,3-dilsopropylethylamine (DIEA), and trifluoromethanesulphonic acid (TMFSA) were obtained from Aldrich Chemical Co. (Milwaukee, WI).

Solid phase peptide synthesis

The thrombin receptor antagonistic peptides, TRAP-1 (H-Ser-Phe-Leu-Leu-Arg-Asn-Pro-OH), and the alanine-scan analogs, TRAP-2 (H-Ser-Ala-Leu-Leu-Arg-Asn-Pro-OH), TRAP-3 (H-Ser-Phe-Ala-Leu-Arg-Asn-Pro-OH), TRAP-4 (H-Ser-Phe-Leu-Ala-Arg-Asn-Pro-OH), TRAP-5 (H-Ser-Phe-Leu-Leu-Ala-Asn-Pro-OH), and TRAP-6 (H-Ser-Phe-Leu-Leu-Arg-Ala-Pro-OH) respectively, were synthesized by 9-fluorenylmethyloxycarbonyl (Fmoc)/Boc solid phase peptide synthesis procedures (Fields and Noble, 1990; Keah et al., 1998; Boysen and Hearn, 2000). The synthesis of TRAP was performed using the Boc-L-Pro-PAM-resin (0.88 mmole/g) at a 0.5-mmol scale using a combined Fmoc/Boc strategy. Typically, the appropriate Boc- or Fmoc-amino acids (3 eq), HOBt (3 eq) and HBTU (3 eq) dissolved in DMF (5 ml) with 0.25 ml DIEA were used. During the synthesis, the presence of free amino groups was monitored by the ninhydrin test (Kaiser et al., 1970). The synthesis was started using Boc-chemistry (TFA deprotection of Pro) with the following two Boc-protected amino acids double-coupled. This double-coupling strategy was predicated on the fact that the extent of deprotection of the first residue, Pro (being a secondary amino acid), cannot be tested with the ninhydrin

reagent, whereas the ninhydrin test gives ambiguous results following deprotection of Asn (and Ser) (Fontenot et al., 1991). After each deprotection with TFA, neutralization was performed with 10% (v/v) DIEA in DMF. Following incorporation of the Asn residue, the synthesis was then based on Fmoc-chemistry with deprotection of the next and subsequent residues achieved with 20% (v/v) piperidine in DMF. Earlier utilization of Fmoc-chemistry in the SPPS inevitably lead to the release of the AsnPro dipeptide from the resin as the cyclic dipeptide diketopiperazine (Fields and Noble, 1990; Bornstein and Balian, 1977).

The synthesis of the Ala-scan TRAP analogs was performed using similar methods, with the exception that a split resin strategy was used, whereby after each coupling the resin was dried and ⅕ of the resin was placed in a separate vessel, prior to coupling the Boc- or Fmoc-Ala residue. The syntheses then proceeded in parallel in an analogous manner to that used for the parent peptide, with the respective peptide-resin repeatedly dried and subdivided until all peptide sequences had been synthesized.

The cleavage of the crude peptide products was performed with TFMSA by incubating 500 mg peptide-resin with 0.25 ml ethane-1,2-dithiol and 0.5 ml thioanisole for 10 min on ice. TFA (5 ml) was added and the mixture incubated for further 10 min on ice. Finally 0.5 ml TFMSA (0.5 ml) was added dropwise and the resulting solution stirred at room temperature for 2 h. After completion of the TFMSA cleavage of the crude peptide products from the resin, the crude peptide was precipitated by the addition of 40 ml cold diethyl ether, the solution stirred for 1 min and then filtered. The precipitate was extracted with 25 ml TFA through the glass sintered filter directly into a round bottom flask. The volume of filtrate was reduced in vacuo with a rotary evaporator (Buchi, Labortechnik AG, Flawil, Switzerland) and again precipitated by adding ice-cold diethylether. The precipitate, containing the crude peptide, was recovered by filtration and the ether disregarded. The precipitate was dissolved in 50% (v/v) acetonitrile/water, lyophilized and the crude peptide stored at 353 K (−20°C).

Peptide purification

The six crude synthetic peptides were each purified by gradient elution reversed-phase high-performance liquid chromatography (RP-HPLC) using a Waters 600/486 HPLC system with a TSK-ODS-120 T column (300 × 21.5 mm inside diameter, Tosoh Corp. Yamaguchi, Japan) packed with 10 μm, 300 Å pore-sized octadecyl silica. The eluents used were: A, 0.1% TFA in water, and B, 0.09% TFA in 60% (v/v) acetonitrile-water, with a linear gradient of 25–75% B over 90 min. Ultraviolet (UV) detection was used at 254 nm except for TRAP-2 (in which Ala replaces Phe[2]) where detection at 214 nm was used. The flow rate was 7.5 ml/min. Because TRAP-1 precipitates in eluent A at high concentrations, this peptide was dissolved in 0.09% TFA, 25% acetonitrile (v/v) in water, and 50–150 mg aliquots were injected. Recovered fractions were analyzed using the Waters 600/486 HPLC system by analytical RP-HPLC and a TSK-ODS-120 T column (150 × 4.6 mm inside diameter, Tosoh Corp.), packed with 5 μm, 300 Å average pore size octadecyl silica. The eluents used were the same as above for the semi-preparative separation, with a linear gradient of 0–100% B over 60 min, UV detection at 214 nm, and a flowrate of 1 ml/min. The molecular masses of the purified peptides were confirmed by electrospray ionization mass spectrometry (ESI-MS) using a Micromass platform (II) quadrupole MS with an electrospray source with Masslynx NT Ver. 3.2 software (Micromass, Cheshire, UK). The synthetic peptides in 50:50 (v/v) ACN/water, with 3% (v/v) formic acid were infused into the instrument at a speed of 10 μl per minute. The ESI-MS spectra of the TRAP peptides were acquired at 343 K at 55V/50V over the mass/charge (m/z) range of 200–2000.

Molecular modeling

Molecular modeling and energy minimization were performed using the CS Chem3D Pro 4.0 software (CambridgeSoft, Corp., Cambridge, MA). Standard molecular dynamics was performed in 10,000 steps by heating the molecule to 600 K at a rate of 1.000 kcal/atom/ps. Energy-minimized structures of each peptide were acquired using the molecular mechanics subroutine MM2 (Allinger, 1977; Allinger et al., 1988; Torrens, 2000) with 2-fs intervals, with average backbone and side-chain conformations determined from the overlap of five acquired structures. The molecular surface area, ΔA_{mol}, solvent accessible surface area, ΔA_{solv}, and hydrophobic surface area, ΔA_{hydr}, of the TRAP peptides (Table 1) in their folded (globular) conformations, and the corresponding surface areas for the TRAP-related peptides in their unfolded conformations, were calculate according to established procedures (Makhatadze and Privalov, 1995; Spassov et al., 1997). The relative hydrophobicities of the TRAP peptide analogs in the presence of immobilized *n*-octyl ligands were calculated according well documented approaches (Wilce et al., 1995).

Instrumental methods

Analytical chromatographic measurements were performed on a Hewlett Packard HP1090 chromatograph and a HP Chemstation (Hewlett Packard, Waldbronn, Germany). All peak profiles were monitored at 215 nm. Temperature was controlled by immersing the analytical columns in a thermostated column coolant-jacket (Alltech Associates, Deerfield, IL) coupled to a recirculating cooler (Colora Messtechnik GmbH, Lorchwutt, Germany). All chromatographic experiments were performed on 150 × 4.6 mm inside diameter Zorbax 300SB-C8 columns (Rockland Technologies, Inc., Littlefalls, DE).

Determination of capacity factor, k', dependencies

Bulk solvents were filtered and degassed by sparging with helium. Capacity factor measurements (Purcell et al., 1999) were performed using water containing 0.09% (v/v) TFA with acetonitrile contents of 14, 15, 16, 17, 18, 19, and 20%, respectively with Zorbax 300SB-C8 columns operated at a flow rate of 1 ml/min and at temperatures of 278–338 K in 5-K increments. Solutions of TRAP-1, -2, -3, -4, -5, and -6 peptides were prepared by dissolving the peptide at a concentration of 1 mg/ml in 0.09% (v/v) TFA in water. The injection size varied between 2.5 and 3.5 μg. Under these concentration and mass loading conditions, the TRAP-1 to TRAP-6 peptides exist as monomeric species. All data points were derived from at least duplicate measurements with retention times between replicates varying typically by less than 1%. The column dead volume was measured as the retention time of the noninteractive solute, sodium nitrate. Various thermodynamic and extra-thermodynamic parameters were calculated using the *Eudoxos* and *Hephaestus* software developed in this laboratory, coupled to the Excel version 5.0 program (Microsoft), whereas the statistical analysis involved the Sigmaplot 4.01 program (Jandel Scientific) linear and nonlinear regression analysis. The relative standard deviations of the replicates for the k' measurements were $\leq \pm 0.6\%$, i.e., the standard deviation of the k' values were smaller than the size of the data points shown in Figs. 1, 2, 4, and 5, respectively. Similarly, the precision in the temperature measurements was $\leq \pm 0.5$ K over the studied temperature range.

RESULTS AND DISCUSSION

General considerations

The extent of binding of a peptide to an immobilized nonpolar ligand as a function of experimental conditions can be evaluated for a reversible, equilibrium interaction from the ratio of the bound-to-free peptide concentration (Hearn, 1998, 2000). When measured with a solid/liquid two-phase

system, such as occurs in membrane-based environments or chromatographic adsorption formats, this concentration dependency can be expressed in terms of the unitless term k', also known as the capacity factor, which is the ratio of the peptide mass bound to the immobilized ligand(s) to the peptide mass in free solution. For convenience, k' is usually expressed as a concentration ratio such that

$$k' = \frac{n_S}{n_M} \times \frac{V_S}{V_M} = K_{assoc} \times \frac{V_S}{V_M} = K_{assoc} \times \Phi, \qquad (1)$$

where n_S and n_M are the number of moles of the peptide in the bound and free states respectively, K_{assoc} is the equilibrium binding constant and Φ the phase ratio of the system, defined as the ratio V_S/V_M, where V_S and V_M are, respectively, the volume of the immobilized ligands/support matrix and the volume of the solvent in the system. Similarly, the dependency of k' on temperature can be evaluated in terms of the respective enthalpic and entropic thermodynamic parameters, such that

$$\ln k' = \frac{-\Delta H^0_{assoc}}{RT} + \frac{\Delta S^0_{assoc}}{R} + \ln \Phi, \qquad (2)$$

where ΔH^0_{assoc} and ΔS^0_{assoc} are the apparent changes in enthalpy and entropy associated with the interaction, R is the universal gas constant, and T is the absolute temperature in degrees Kelvin. The equilibrium binding behavior of a large number of ligands for G-protein coupled receptors and ligand-gated ion channel receptors have recently been analyzed in considerable detail based on these relationships (Borea et al., 2000), revealing that the discrimination of various agonists/antagonists mechanistically appears to be a consequence of the thermodynamic reorganization of solvent molecules that occur during the binding. Analogous situations occur when peptide agonists/antagonists interact with immobilized nonpolar *n*-alkyl or phospholipid ligand(s). When this interaction is an isothermic and isobaric (constant pressure) process, linear van't Hoff plots are anticipated, with the change in heat capacity, ΔC^0_p, equalling zero (Boysen et al., 1999; Hearn et al., 1999). However, when the interaction follows a homothermic or heterothermic process, curvilinear van't Hoff plots are anticipated whereby $\Delta C^0_p \neq 0$ and is a function of T (Boysen et al., 1999; Hearn et al., 1999). Although fitting of experimental data to the linear form of the van't Hoff dependency has often been used in studies related to the thermal stability of proteins in bulk solution, differential scanning and isothermal titration microcalorimetric studies with proteins bound to chemical defined surfaces or undergoing ligand-binding events have shown that the temperature dependence of ΔC^0_p is often associated with dome-shaped (or inverted dome-shaped) dependencies of the logarithmic equilibrium association constant, $\ln K_{assoc}$ (or ΔG^0_{assoc}) on temperature (Klotz, 1999). Similarly, nonlinear van't Hoff behavior has been observed for peptides and proteins in both reversed-phase and hydrophobic interaction chromatographic systems. Such behavior can be approximated (Melander et al., 1984; Vailaya and Horvath, 1996; Haidacher et al., 1996; Hearn, 2001a) as a quadratic relationship linking k' and the temperature, T,

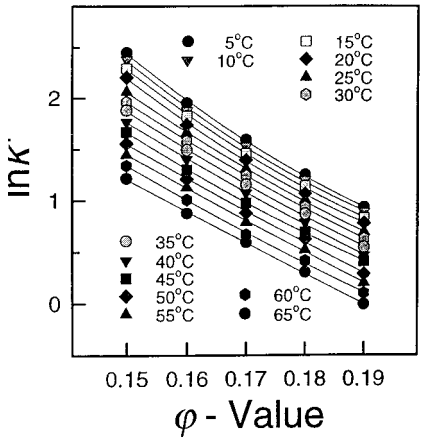

FIGURE 1 Plots of logarithmic capacity factor, $\ln k'$, versus the volume fraction of organic solvent, φ, for the TRAP-1 at different temperatures from 278 to 338 K (5–65°C).

$$\ln k' = b_{(0)} + \frac{b_{(1)}}{T} + \frac{b_{(2)}}{T^2} + \ln \Phi. \qquad (3)$$

Hence, from Eqs. 1 and 2, the change in enthalpy, ΔH^0_{assoc}, can be expressed as

$$\Delta H^0_{assoc} = -R\left[b_{(1)} + \frac{2b_{(2)}}{T}\right], \qquad (4)$$

whereas the change in entropy, ΔS^0_{assoc}, is given by

$$\Delta S^0_{assoc} = R\left[b_{(0)} - \frac{b_{(2)}}{T^2}\right], \qquad (5)$$

and the change in heat capacity, ΔC^0_p, is given by

$$\Delta C^0_p = R\left[\frac{2b_{(2)}}{T^2}\right], \qquad (6)$$

where $b_{(0)}$, $b_{(1)}$, and $b_{(2)}$ are steri-electronic parameters specific for the structure of the peptide (or protein). In the present investigation, the interactive behavior of a series of TRAP-related peptide analogs with immobilized *n*-octyl ligands has been evaluated according to Eqs. 1–6 from the corresponding $\ln k'$ versus $1/T$ plots measured under reversible, equilibrium-binding conditions at fixed solvent composition(s). This analysis permits the respective thermodynamic parameters associated with the interaction to be derived and quantified, and the related extra-thermodynamic dependencies to be evaluated in terms of corresponding structural relationships.

Figure 1 shows the plot of the logarithmic capacity factor, $\ln k'$, of TRAP-1 versus the volume fraction of acetonitrile,

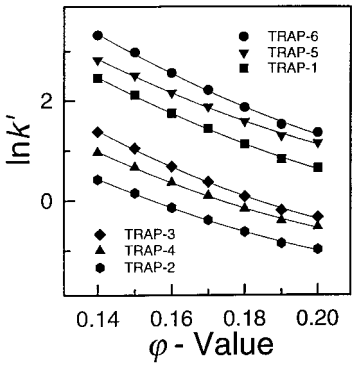

FIGURE 2 Plots of the logarithmic capacity factor, ln k', versus the volume fraction of organic solvent, φ, for the alanine-scan TRAP peptides, TRAP-2–6 at 298 K.

φ, for water-acetonitrile mixtures of different acetonitrile contents over the temperature range 278–338 K. The experimental data obtained were fitted to first and second order dependencies of ln k' on φ, with regression coefficients falling within the range of $r^2 = 0.9902–0.9992$ for the first-order fit and $r^2 = 0.9983–0.9999$ for the second order fit. The higher correlation coefficients observed when the TRAP-1 data were fitted to quadratic dependencies of ln k' on φ are consistent with the well-known parabolic binding relationship for polypeptides and proteins on adsorption to immobilized *n*-alkyl ligands from aquo-organic solvent mixtures (Hearn et al., 1999, 2001a) Similarly, the corresponding plots at 298 K for the TRAP 1–6 peptides where, in all cases, the ln k' versus φ plots were curvilinear (Fig. 2).

For the TRAP-1 peptide, and for the Ala-scan analogs, the expected hydrophobic interaction mechanism for the peptide–nonpolar ligand interaction was observed, with decreases in ln k' values as the φ value was increased. The relative trend for the binding of the TRAP-1 analogs was in agreement with the effect anticipated for amino acid substitution, i.e., the substitution of a more hydrophobic residue by a less hydrophobic residue in TRAP-2, TRAP-3, and TRAP-4 leads to smaller k' values, whereas the replacement of a charged or polar residue in TRAP-5 and TRAP-6 by the alanine residue results in an increase in the k' value as compared to the naturally occurring TRAP-1 (cf. Table 1).

The results from the molecular modeling and associated energy minimization studies indicated that all TRAP analogs have globular shape, assuming that a local minimum not an absolute minimum was found. These investigations show that TRAP-1 has a hydrophobic face consisting of Phe^2, Leu^3, and Pro^7. In Fig. 3 *A* is shown an overlay presentation of five randomly selected energy-minimized conformational structures for TRAP-1, having energy minima between 63.1 and 73.8 kcal/mol. As evident from Fig. 3 *A*, the *N*-termini can be overlayed very well, with the Phe^2 side chain of the peptide with the lowest energy minimum closest to the core, whereas the C-termini with the Pro^7 are more flexible. In Fig. 3 *B* is shown the overlay presentation for energy-minimized conformational structures for TRAP-1, TRAP3, TRAP-4, and TRAP 5, where the Phe^2 and Pro^7 side chains are in close proximity. Although the

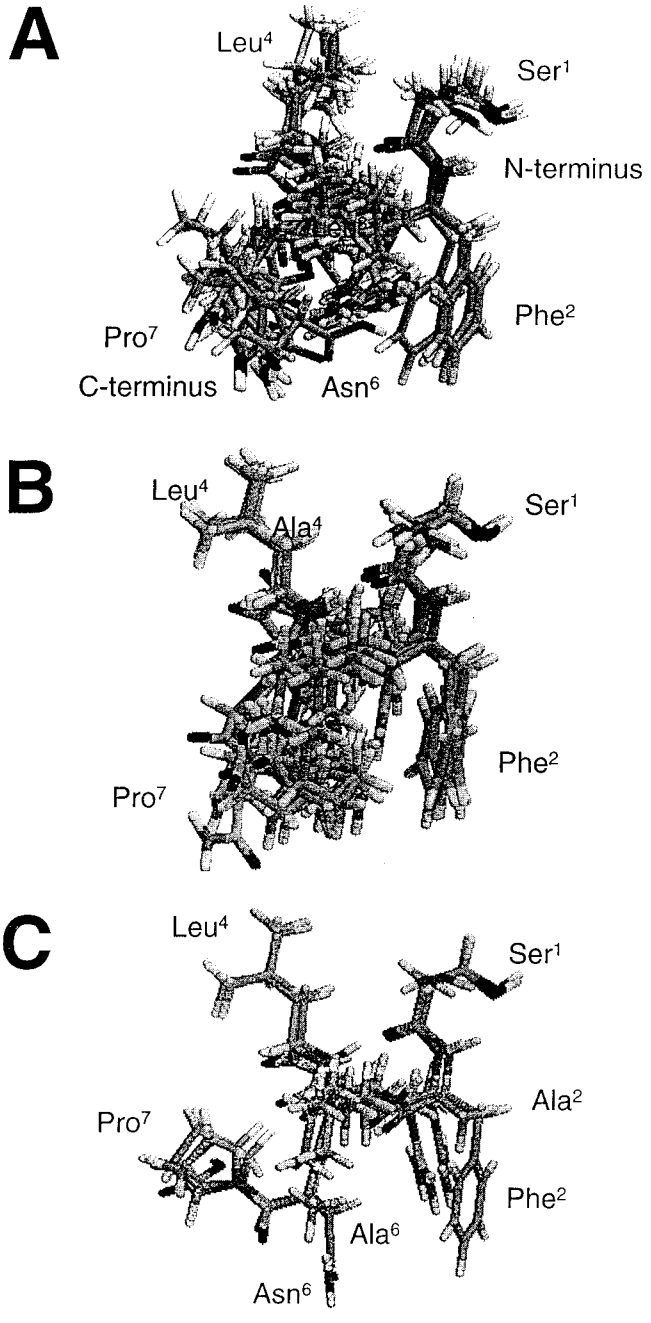

FIGURE 3 (*A*) Overlay presentation for five simulated energy-minimized conformer structures for TRAP-1. (*B*) Overlay presentation of TRAP and TRAP-related analogs TRAP-3, TRAP-4, and TRAP-5 with Phe^2 and Pro^7 side chains in close proximity. (*C*) Overlay presentation of TRAP-2 and TRAP-6 with the side chain of Pro^7 distal to the side chain of Phe^2.

N-termini and the residues at position 1, 2, and 4 are in good alignment for these peptides, the location of the C-termini varies according to the position of the Ala substitution. The corresponding overlay presentation for the simulated energy-minimized conformational structures for TRAP-2 and TRAP-6, where the Pro^7 side chain is distal to the Phe^2 side chain, is shown in Fig. 3 *C*. Here, the Ala substitution of the Phe residue has virtually no impact on the rest of the molecule. However, as will be discussed later, the thermodynamic data for both peptides revel that they behave differently in response to increasing temperature.

The strength of binding of TRAP-1 and the Ala-scan analogs to the immobilized *n*-octyl ligands, expressed in terms of the relative K_{assoc} or ln k' values, is largely in agreement with the relative hydrophobicity values calculated for these peptides according to the procedures of Wilce et al. (Wilce et al., 1995) (cf. Table 1). TRAP-3 and TRAP-4 have identical amino acid compositions but different amino acid sequences with respect to positions 3 and 4 and nominally have the same relative hydrophobicity. However, as apparent from the ln k' versus φ plots (Fig. 1 and 2) these peptides differ in terms of their equilibrium binding constants with the immobilised *n*-octyl ligands. The reason for this difference becomes apparent when their possible structures, derived by molecular modeling methods, are examined. According to the molecular modeling results, TRAP-4 is the far more compact molecule, with Pro^2, Leu^3 and Phe^2 collectively generating a hydrophobic patch, only part of which can be accessed by the immobilized *n*-octyl ligands. In contrast, TRAP-3 has the more open structure with Leu^4 and Pro^7 in distal positions with the hydrophobic patch associated with the Phe^2 residue also more accessible to the immobilized *n*-octyl ligands. This structure–interaction correlation is in agreement with the observed changes in heat capacity of these peptides (as discussed later).

van't Hoff measurements

The van't Hoff plots for TRAP-1 determined at different φ-values with water-acetonitrile mixtures containing 0.09% TFA are shown in Fig. 4. In all cases, for an individual TRAP peptide examined in different solvent compositions or with different TRAP peptides using the same solvent composition, the correlation coefficients for the second-order fit of the experimental data to the dependency of ln k' on $1/T$ were significantly higher than for a first-order fit (cf. Tables 2 and 3) at both the 95% and 99% confidence intervals. Thus, the van't Hoff data for TRAP-1 in different solvent compositions followed a quadratic relationship as given by Eq. 3, e.g., when $\varphi = 0.17$, the correlation coefficient was $r^2 = 0.9995$ at a 95% confidence level, with significantly lower correlation coefficients determined when the ln k' versus $1/T$ data for TRAP-1 was fitted to a first-order approximation for a defined φ-value over the same temperature ranges. Consequently, the van't Hoff dependencies of TRAP-1 can be described in terms of heterothermic processes (Boysen et al., 1999; Hearn and Zhao, 1999; Hearn 2001a) with ΔH^0_{assoc}, ΔS^0_{assoc} and ΔC^0_p all dependent on *T*. As evident from Fig. 5, analogous nonlinear van't Hoff behavior was also evident in all cases for the Ala-scan TRAP analogs at a defined value of φ, for example at $\varphi = 0.14$.

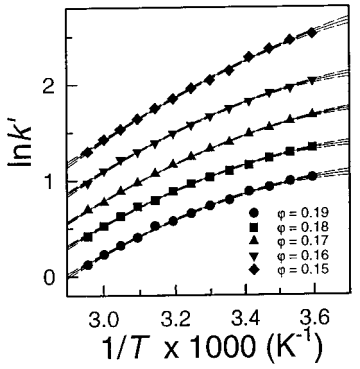

FIGURE 4 Plots of the logarithmic capacity factor, ln k', versus $1/T$ for TRAP-1 at different φ values with the experimental data fitted to a second-order polynomial function (*solid lines*) with the 95% confidence intervals depicted as dotted lines. The correlation coefficients for these second-order fit and the corresponding first-order fit of the experimental ln k' versus $1/T$ data are listed in Table 2.

Changes in the entropy and enthalpy of association for the TRAP-peptide–nonpolar ligand interaction

The respective values of ΔH^0_{assoc} and ΔS^0_{assoc} for TRAP and the Ala-scan analogs as a function of *T* and φ were calculated according to Eqs. 3–5 and the results are shown in Fig. 6, 7, and Table 4. Thus, at 318 K and $\varphi = 0.17$, the values of ΔH^0_{assoc} and ΔS^0_{assoc} for TRAP-1 were -13.31 ± 0.03 kJ·mol^{-1} and -32.86 ± 0.10 Jmol^{-1}·K^{-1}, respectively, with the results obtained for TRAP-1 (and the other peptides)

TABLE 2 The correlation coefficients for a linear and quadratic fit of the corresponding experimental data to the dependency of ln k' versus $1/T$ for TRAP-1 at different φ values as shown in Figure 4

	Correlation Coefficient, r^2	
φ-Value	Linear Fit	Quadratic Fit
0.19	0.9760	0.9987
0.18	0.9774	0.9991
0.17	0.9842	0.9995
0.16	0.9829	0.9992
0.15	0.9918	0.9991

For all five plots, the second-order fit resulted in higher correlation coefficients at both the 95 and 99% confidence interval than the first-order fit, with differences ranging from 0.0073 to 0.0227.

TABLE 3 The correlation coefficients and 95% confidence intervals for a linear and quadratic fit of the experimental ln k' versus $1/T$ data for TRAP-1 and its Alanine-scan peptide analogs at $\varphi = 0.14$ corresponding to the data shown in Fig. 5

First Order Fit of the ln k' versus $1/T * 1000$ (K^{-1}) Data						
TRAP Peptide	Variables			95% Confidence Intervals		
	Slope	Y-Intercept	X-Intercept	Slope	Y-Intercept	r^2
6	2.011 ± 0.1428	−3.449 ± 0.4659	1.715	1.697 to 2.325	−4.474 to −2.423	0.9475
5	1.526 ± 0.140	−2.339 ± 0.457	1.533	1.218 to 1.834	−3.344 to −1.334	0.9153
1	2.027 ± 0.146	−4.307 ± 0.477	2.124	1.706 to 2.349	−5.356 to −3.258	0.9460
3	1.916 ± 0.111	−5.079 ± 0.361	2.651	1.672 to 2.159	−5.874 to −4.284	0.9646
4	1.641 ± 0.144	−4.493 ± 0.469	2.739	1.325 to 1.957	−5.524 to −3.462	0.9223
2	1.027 ± 0.176	−2.893 ± 0.574	2.818	0.6392 to 1.414	−4.157 to −1.629	0.7556
Second Order Fit of the ln k' versus $1/T * 1000$ (K^{-1}) Data						
TRAP Peptide	Variables			95% Confidence Intervals		
	A	B	C	A	B	C	r^2
6	−30.95	18.89	−2.579	−36.49 to −25.42	15.49 to 22.28	−3.098 to −2.061	0.9960
5	−28.61	17.65	−2.464	−35.50 to −21.72	13.42 to 21.87	−3.109 to −1.819	0.9897
1	−32.05	19.05	−2.602	−38.60 to −25.50	15.04 to 23.06	−3.215 to −1.989	0.9946
3	−24.37	13.75	−1.809	−32.08 to −16.66	9.027 to 18.48	−2.531 to −1.087	0.9914
4	−29.61	17.05	−2.356	−39.49 to −19.73	11.00 to 23.11	−3.281 to −1.430	0.9816
2	−35.19	20.84	−3.029	−45.18 to −25.20	14.72 to 26.97	−3.964 to −2.093	0.9606

The resulting plots of the enthalpy of interaction, ΔH^0_{assoc}, entropy of interaction, ΔS^0_{assoc}, heat capacity, ΔC^0_p, and Gibbs free energy of interaction, ΔG^0_{assoc}, versus T, derived from these first- and second-order regression analyses for TRAP-1 and its analogs are depicted in Figs. 6 and 7, respectively.

under the different temperature and solvent conditions similarly exhibiting narrow confidence intervals. As evident from Figs. 6 *A* and 7 *A*, the TRAP-1 peptide–ligand interaction was enthalpically-driven over the temperature range of 278–358 K, with ΔH^0_{assoc} progressively becoming more negative as T was increased. Moreover, the ΔH^0_{assoc} values for the interaction of the TRAP peptides with the immobilized *n*-octyl ligands were more negative for solvent mixtures of higher water content (Fig. 6 *A*). The heat required for (partial) dehydration of the TRAP peptides prior to or during adsorption to the immobilized *n*-octyl ligands differs for the different peptides (Fig. 7 *A*), i.e., the heat required under low temperature conditions (278 K) to dehydrate the most hydrophilic peptide (TRAP-2) was ~10–15 kJmol^{-1} higher than that required to dehydrate the other more hydrophobic TRAP peptides. Both ΔH^0_{assoc} and ΔS^0_{assoc} were temperature dependent with the TRAP peptides exhibiting characteristic compensation temperatures given by T_H (where $\Delta H^0_{assoc} = 0$) and T_S (where $\Delta S^0_{assoc} = 0$). When the ΔH^0_{assoc} values for the TRAP peptides obtained from these van't Hoff plots are compared to related studies (Lin et al., 2001), based on isothermal titration microcalorimetric procedures, for the determination of the adsorption enthalpy of peptides and proteins when bound to immobilized *n*-alkyl ligands, similar dependencies of ΔH^0_{assoc}, and hence ΔC^0_p, on T are evident at comparable solute concentrations. Compared to large polypeptides or small proteins where ΔH^0_{assoc} differences of between 100 and 200 kJmol^{-1} have been observed under similar adsorption conditions over the same temperature range of 278–338 K, the changes in ΔH^0_{assoc} values for a specific TRAP peptide were relatively small, i.e., $\Delta\Delta H^0_{assoc} \approx$ 15–30 kJmol^{-1} over this temperature range, values that are consistent with the small molecular size, composition and solvational potential of these peptides.

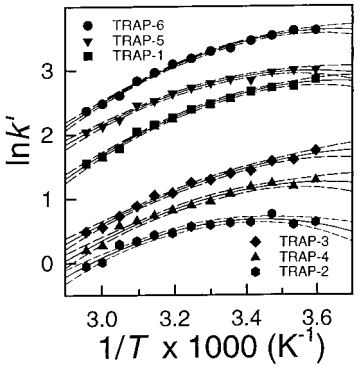

FIGURE 5 Plots of the logarithmic capacity factor, ln k', versus $1/T$ for TRAP-1 and its alanine-scan peptide analogs at $\varphi = 0.14$ with the experimental data fitted to a second-order polynomial function (*solid lines*) with the 95% confidence intervals depicted as dotted lines. The correlation coefficients for these second-order fit and the corresponding first-order fit of the experimental ln k' versus $1/T$ data are listed in Table 3.

As evident from Fig. 8, the interaction of TRAP-1 with the *n*-octyl ligands involves an entropy–enthalpy compensation phenomenon at different solvent compositions. Entropy-enthalpy compensation was also observed for the TRAP Ala-scan analogs. Such behavior is consistent with these peptide–ligand systems involving participation of

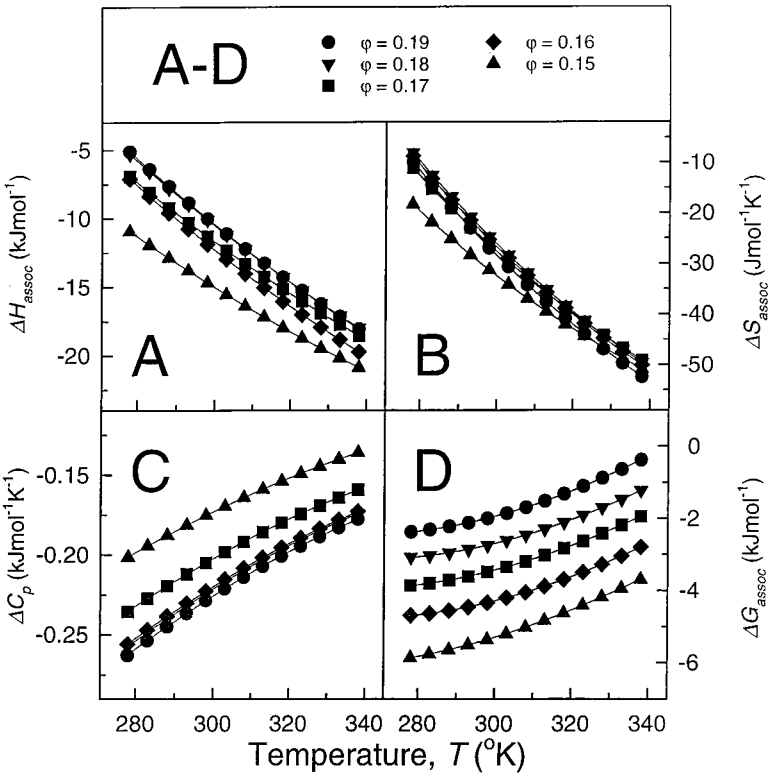

FIGURE 6 Plots of (*A*) the change in enthalpy ΔH^0_{assoc} versus T; (*B*) the change in entropy ΔS^0_{assoc} versus T; (*C*) the change heat capacity ΔC^0_p versus T; and (*D*) the change in Gibbs free energy ΔG^0_{assoc} versus T for the TRAP-1 peptide at different φ values.

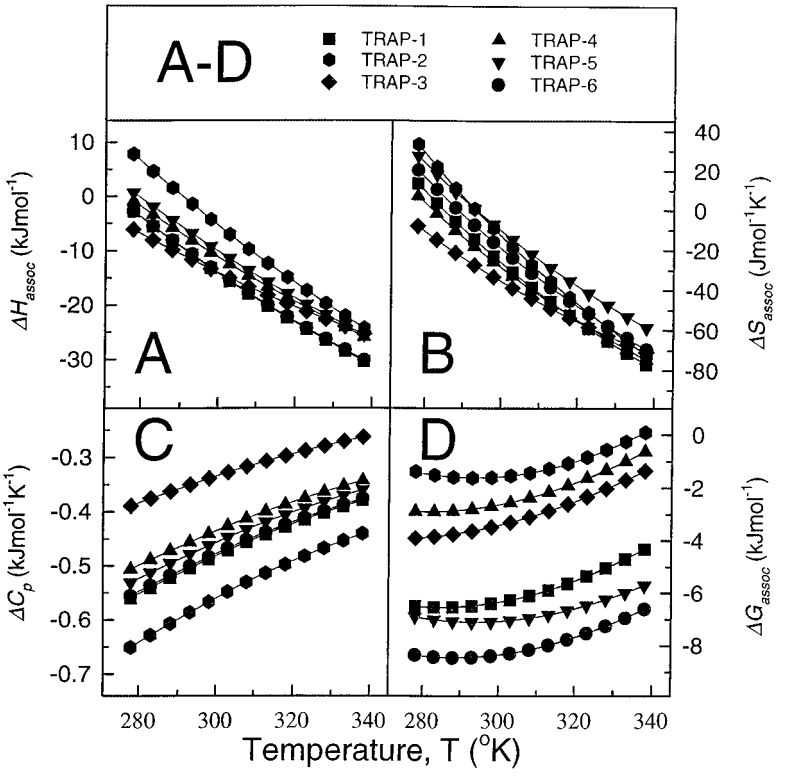

FIGURE 7 Plots of (*A*) the change in enthalpy ΔH^0_{assoc} versus T; (*B*) the change in entropy ΔS^0_{assoc} versus T; (*C*) the change heat capacity ΔC^0_p versus T; and (*D*) the change in Gibbs free energy ΔG^0_{assoc} versus T for the TRAP-1 and its Alanine-scan peptide analogs at $\varphi = 0.14$.

TABLE 4 The slopes and 95% confidence intervals of the dependence of the enthalpy of interaction, ΔH^0_{assoc}, entropy of interaction, ΔS^0_{assoc}, heat capacity, ΔC^0_p, and Gibbs free energy of interaction, ΔG^0_{assoc}, on temperature for TRAP-1 and its alanine scan peptide analogs at $\varphi = 0.14$, based on a first- and second-order fit of the experimental ln k' versus $1/T$ data shown in Fig. 5

A Enthalpy, ΔH^0_{assoc} (kJmol^{-1}) versus Temperature, T (K)

	First-Order Fit of the ln k' versus $1/T * 1000$ (K^{-1}) Data*		Second-Order Fit of the ln k' versus $1/T * 1000$ (K^{-1}) Data†	
TRAP	Slope‡	95% Confidence Interval of Slope	Slope $\times 10^2$	95% Confidence Interval of Slope $\times 10^2$
6	0	n.d.§	−45.55 ± 0.74	−43.91 to −47.18
5	0	n.d.	−43.57 ± 0.71	−42.01 to −45.13
1	0	n.d.	−45.90 ± 0.75	−44.26 to −47.55
3	0	n.d.	−31.89 ± 0.52	−30.75 to −33.04
4	0	n.d.	−41.52 ± 0.68	−40.03 to −43.01
2	0	n.d.	−53.38 ± 0.87	−51.47 to −55.30

B Entropy, ΔS^0_{assoc} (Jmol^{-1}K^{-1}) versus Temperature, T (K)

	Slope	95% Confidence Interval of Slope	Slope	95% Confidence Interval of Slope
6	0	n.d.	−1.49 ± 0.04	−1.41 to −1.57
5	0	n.d.	−1.42 ± 0.03	−1.35 to −1.50
1	0	n.d.	−1.50 ± 0.04	−1.42 to −1.58
3	0	n.d.	−1.04 ± 0.03	−0.99 to −1.10
4	0	n.d.	−1.36 ± 0.03	−1.28 to −1.43
2	0	n.d.	−1.75 ± 0.04	−1.65 to −1.84

C Heat capacity, ΔC^0_p (kJmol^{-1}K^{-1}) versus Temperature, T (K)

	Slope $\times 10^4$	95% Confidence Interval of Slope $\times 10^4$	Slope $\times 10^3$	95% Confidence Interval of Slope $\times 10^3$
6	1.78 ± 0.04	1.69 to 1.87	2.98 ± 0.07	2.82 to 3.14
5	1.34 ± 0.05	1.22 to 1.46	2.85 ± 0.07	2.70 to 3.00
1	1.88 ± 0.05	1.78 to 1.98	3.02 ± 0.07	2.84 to 3.16
3	1.62 ± 0.04	1.52 to 1.71	2.08 ± 0.05	1.97 to 2.20
4	1.44 ± 0.04	1.34 to 1.54	2.72 ± 0.07	2.57 to 2.87
2	0.95 ± 0.05	0.84 to 1.05	3.49 ± 0.09	3.31 to 3.68

D Gibbs free energy, ΔG^0_{assoc} (kJmol^{-1}) versus Temperature, T (K)

	Slope $\times 10^3$	95% Confidence Interval of Slope $\times 10^3$	Slope $\times 10^3$	95% Confidence Interval of Slope $\times 10^3$
6	28.67 ± 4.45	19.76 to 37.58	29.77 ± 3.71	21.61 to 37.94
5	19.44 ± 4.19	11.06 to 27.89	20.50 ± 3.55	12.67 to 28.32
1	35.80 ± 2.28	31.24 to 40.66	36.91 ± 3.74	28.68 to 45.15
3	42.22 ± 4.45	34.36 to 52.32	42.99 ± 2.60	37.27 to 48.71
4	37.35 ± 4.64	28.05 to 46.75	38.36 ± 3.39	30.91 to 45.81
2	24.07 ± 4.53	14.90 to 33.23	25.37 ± 4.35	15.79 to 34.94

In the case of a linear dependence of ln k' on $1/T$, ΔH^0_{assoc} and ΔS^0_{assoc} are expected to be independent of T, and thus, theoretically, the slopes of the plots of ΔH^0_{assoc} versus T and ΔS^0_{assoc} versus T should be zero as observed from the data analysis using the GraphPad Prism version 2.01 software package (Graphpad, San Diego, CA) for statistical analysis.

*Data fitted according to $\ln k' = b_{(0)} + b_{(1)}/T + \ln \Phi$.

†Data fitted according to $\ln k' = b_{(0)} + b_{(1)}/T + b_{(2)}/T^2 + \ln \Phi$.

‡The Prism software package reported this as a horizontal line of slope equal to zero.

§n.d., Not calculated by the statistical analysis package.

multiple, weak, intermolecular forces (Dunitz, 1995). The results indicate that the binding of TRAP 1–6 peptides within this interactive molecular system (including solvent) was generally exothermic (i.e., involved a negative ΔH^0_{assoc} under most conditions) but was compensated by a decrease in ΔS^0_{assoc} that results from the reduced molecular flexibility of the peptide on binding to the immobilized *n*-octyl ligands. As the temperature was increased, the TRAP-related peptides and the *n*-octyl ligands are progressively solvated to a greater extent, resulting in smaller contact areas, and thus reduced association between the peptides with the nonpolar environment of the *n*-octyl ligands.

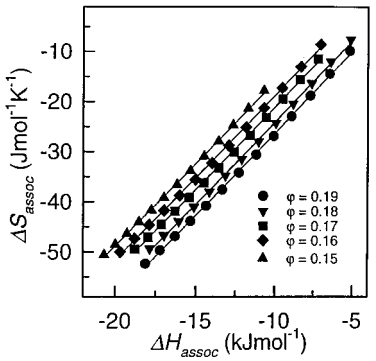

FIGURE 8 Plot of the change in entropy ΔS^0_{assoc} versus the change in enthalpy ΔH^0_{assoc} for the TRAP-1 peptide at different φ values.

Changes in the heat capacity of association for the TRAP peptide–nonpolar ligand interaction

Another thermodynamic parameter important for characterizing the TRAP–*n*-octyl ligand interaction is the change in heat capacity, ΔC^0_p, with an increase in the extent of burial of hydrophobic surfaces in a nonpolar environment yielding a more negative value of ΔC^0_p (Ross and Rekharsky, 1996). It is widely accepted that ΔC^0_p is proportional to the accessible surface area of a peptide or protein, which can be partitioned into an apolar surface (with the energetics related to the hydrophobic effect) or into a polar surface (where the energetics are predominantly related to hydrogen-bonding effects) (Murphy and Gill, 1991; Murphy, 1999). To assess the nature of the dependence of ΔC^0_p on temperature for these TRAP peptides, the experimental data used for the generation of the ln k' versus $1/T$ plots for TRAP-1 at different solvent compositions and for TRAP-1–Trap-6 at $\varphi = 0.14$ were fitted to the relevant equations with and without ΔC^0_p having a temperature dependence, i.e., ln k' fitted as a first-order or second-order dependence on $1/T$. These results are found in Table 3–6.

Figure 6 *C* shows that the change in ΔC^0_p for TRAP-1–*n*-octyl ligand interaction was negative under all solvent conditions as expected for a hydrophobic interaction process. Thus, at 318 K and $\varphi = 0.17$, the value of ΔC^0_p for TRAP-1 was -0.192 ± 0.002 kJmol^{-1}·K^{-1}. Moreover, the corresponding ΔC^0_p values for TRAP-1 obtained under the other temperature and solvent conditions or the related analogs obtained at $\varphi = 0.14$ similarly exhibiting negative values with small standard deviations at the 95% and 99% confidence intervals for second-order fit of the experimental data (Table 4 and 6) for the ln k' dependency on $1/T$ according to Eq. 3. In all cases, the ΔC^0_p values followed the important criterion of being $\neq 0$ and < 0 under the experimental conditions investigated with the ΔC^0_p values (Figs. 6 *C* and 7 *C*) becoming more positive at higher temperatures, indicating a decrease in the hydrophobic contact area associated with the peptide–nonpolar ligand interaction. This behavior was also paralleled by changes in the Gibbs free energy, ΔG^0_{assoc}, as the temperature was increased (Figs. 6 *D* and 7 *D*). Thus, the plots of ΔG^0_{assoc} versus T for these TRAP-related peptides confirm that their interaction with the *n*-octyl ligands was spontaneous at all temperatures, but their interactions became less favorable at more elevated temperatures. These findings indicate a small but nevertheless significant dependence of ΔC^0_p values (e.g., ≈ -0.13 kJmol^{-1}K^{-1} $\pm$ 0.01 $\leq \Delta C^0_p \leq -0.27$ kJmol^{-1}K^{-1} $\pm$ 0.01) on the temperature over the range of

TABLE 5 The correlation coefficients and 95% confidence intervals for a linear and quadratic fit of the experimental ln k' versus $1/T$ data for TRAP-1 at different φ values, corresponding to the data shown in Fig. 4

First Order Fit of the ln k' versus $1/T * 1000$ (K^{-1}) Data						
TRAP-1	Variables			95% Confidence Intervals		
φ Value	Slope	Y-Intercept	X-Intercept	Slope	Y-Intercept	r^2
0.19	1.410 ± 0.067	−3.968 ± 0.219	2.813	1.263 to 1.558	−4.449 to −3.486	0.9757
0.18	1.416 ± 0.065	−3.685 ± 0.212	2.602	1.274 to 1.559	−4.151 to −3.220	0.9775
0.17	1.546 ± 0.059	−3.817 ± 0.193	2.469	1.416 to 1.676	−4.242 to −3.392	0.9841
0.16	1.629 ± 0.065	−3.754 ± 0.212	2.305	1.486 to 1.772	−4.221 to −3.287	0.9828
0.15	1.925 ± 0.053	−4.327 ± 0.172	2.248	1.809 to 2.041	−4.706 to −3.948	0.9918
Second Order Fit of the ln k' versus $1/T * 1000$ (K^{-1}) Data						
TRAP-1	Variables			95% Confidence Intervals		
φ Value	A	B	C	A	B	C	r^2
0.19	−17.05	9.435	−1.226	−19.23 to −14.86	8.095 to 10.78	−1.431 to −1.022	0.9987
0.18	−16.42	9.232	−1.195	−18.22 to −14.63	8.131 to 10.33	−1.363 to −1.026	0.9991
0.17	−15.48	8.705	−1.094	−16.96 to −14.01	7.804 to 9.607	−1.232 to −0.9565	0.9995
0.16	−16.45	9.419	−1.191	−18.48 to −14.42	8.177 to 10.66	−1.380 to −1.001	0.9992
0.15	−14.28	8.035	−0.9339	−16.79 to −11.78	6.501 to 9.569	−1.168 to −0.6995	0.9991

The resulting plots of the enthalpy of interaction, ΔH^0_{assoc}, entropy of interaction, ΔS^0_{assoc}, heat capacity, ΔC^0_p, and Gibbs free energy of interaction, ΔG^0_{assoc}, versus T, derived from these first- and second-order regression analyses for TRAP-1 and its analogs are depicted in Fig. 6 and 7, respectively.

TABLE 6 The slopes and 95% confidence intervals of the dependence of the enthalpy of interaction, ΔH^0_{assoc}, entropy of interaction, ΔS^0_{assoc}, heat capacity, ΔC^0_p, and Gibbs free energy of interaction, ΔG^0_{assoc}, on temperature for TRAP-1 peptide at different φ values, based on a first- and second-order fit of the experimental ln k' versus 1/T data shown in Fig. 6

A Enthalpy, ΔH^0_{assoc} (kJmol^{-1}) versus Temperature, T (K)				
	First-Order Fit of the ln k' versus $1/T * 1000$ (K^{-1}) Data*		Second-Order Fit of the ln k' versus $1/T * 1000$ (K^{-1}) Data†	
φ Value	Slope‡	95% Confidence Interval of Slope	Slope $\times 10^2$	95% Confidence Interval of Slope $\times 10^2$
0.19	0	n.d.§	−21.54 ± 0.35	−22.31 to −20.77
0.18	0	n.d.	−21.12 ± 0.35	−21.87 to −20.36
0.17	0	n.d.	−19.31 ± 0.32	−20.00 to −18.62
0.16	0	n.d.	−20.98 ± 0.34	−21.73 to −20.23
0.15	0	n.d.	−16.52 ± 0.27	−17.11 to −0.16
B Entropy, ΔS^0_{assoc} (Jmol^{-1}K^{-1}) versus Temperature, T (K)				
	Slope	95% Confidence Interval of Slope	Slope	95% Confidence Interval of Slope
0.19	0	n.d.	−0.70 ± 0.02	−0.74 to −0.67
0.18	0	n.d.	−0.69 ± 0.02	−0.73 to −0.65
0.17	0	n.d.	−0.63 ± 0.02	−0.67 to −0.60
0.16	0	n.d.	−0.69 ± 0.02	−0.72 to −0.65
0.15	0	n.d.	−0.54 ± 0.01	−0.57 to −0.51
C Heat capacity, ΔC^0_p (kJmol^{-1}K^{-1}) versus Temperature, T (K)				
	Slope $\times 10^4$	95% Confidence Interval of Slope $\times 10^4$	Slope $\times 10^3$	95% Confidence Interval of Slope $\times 10^3$
0.19	1.21 ± 0.049	1.10 to 1.32	1.40 ± 0.04	1.36 to 1.48
0.18	1.28 ± 0.048	1.17 to 1.38	1.38 ± 0.03	1.31 to 1.45
0.17	1.33 ± 0.050	1.22 to 1.44	1.26 ± 0.03	1.20 to 1.32
0.16	1.44 ± 0.053	1.32 to 1.56	1.37 ± 0.03	1.29 to 1.44
0.15	1.80 ± 0.044	1.70 to 1.90	1.08 ± 0.02	1.02 to 1.13
D Gibbs free energy, ΔG^0_{assoc} (kJmol^{-1}) versus Temperature, T (K)				
	Slope $\times 10^3$	95% Confidence Interval of Slope $\times 10^3$	Slope $\times 10^3$	95% Confidence Interval of Slope $\times 10^3$
0.19	32.98 ± 0.00	n.d.	33.52 ± 1.75	29.66 to 37.38
0.18	30.63 ± 0.00	n.d.	31.15 ± 1.72	27.36 to 34.93
0.17	31.75 ± 0.00	n.d.	32.22 ± 1.57	28.75 to 35.68
0.16	31.22 ± 0.00	n.d.	31.74 ± 1.71	27.97 to 35.51
0.15	35.97 ± 0.00	n.d.	36.37 ± 1.35	33.41 to 39.33

In the case of a linear dependence of ln k' on 1/T, ΔH^0_{assoc} and ΔS^0_{assoc} are expected to be independent of T, and thus, theoretically, the slopes of the plots of ΔH^0_{assoc} versus T and ΔS^0_{assoc} versus T should be zero as observed from the data analysis using the GraphPad Prism version 2.01 software package (Graphpad, San Diego, CA) for statistical analysis.

*Data fitted according to $\ln k' = b_{(0)} + b_{(1)}/T + \ln \Phi$.

†Data fitted according to $\ln k' = b_{(0)} + b_{(1)}/T + b_{(2)}/T^2 + \ln \Phi$.

‡The Prism software package reported this as a horizontal line of slope equal to zero.

§n.d., Not calculated by the statistical analysis package.

278–338 K for TRAP-1 and its Ala-scan analogs and are consistent with the small molecular size and lack of well-developed secondary structure of these peptides under these experimental conditions. These ΔC^0_p values are comparable in value to ΔC^0_p for the highly stabilized equine cytochrome c ($\Delta C^0_p \approx -0.9$ kJmol^{-1}K^{-1}) (R. I. Boysen, A. J. O. Jong and M. T. W. Hearn, in preparation) but are significantly smaller than found for the interaction of multimeric coiled-coil polypeptides, such as the transcription factors *c-Jun* or *c-Fos*, with nonpolar ligands, i.e., $\Delta C^0_p \approx -43.8$ kJmol^{-1}K^{-1} for the interactions of this coiled-coil polypeptide with *n*-octyl ligands under similar experimental conditions (Boysen et al., 2002). In this latter case with the homo- or hetero- *c-Jun* or *c-Fos* dimers, the experimental findings have documented that a two-state unfolding process occurs with the coiled coil *c-Jun/c-Fos* polypeptide dimers first uncoiling and the individual α-helical coils then transitioning toward random coil structures with large incremental changes in ΔC^0_p arising as the temperature was increased. Beside the overall trends in the ΔC^0_p values of the TRAP

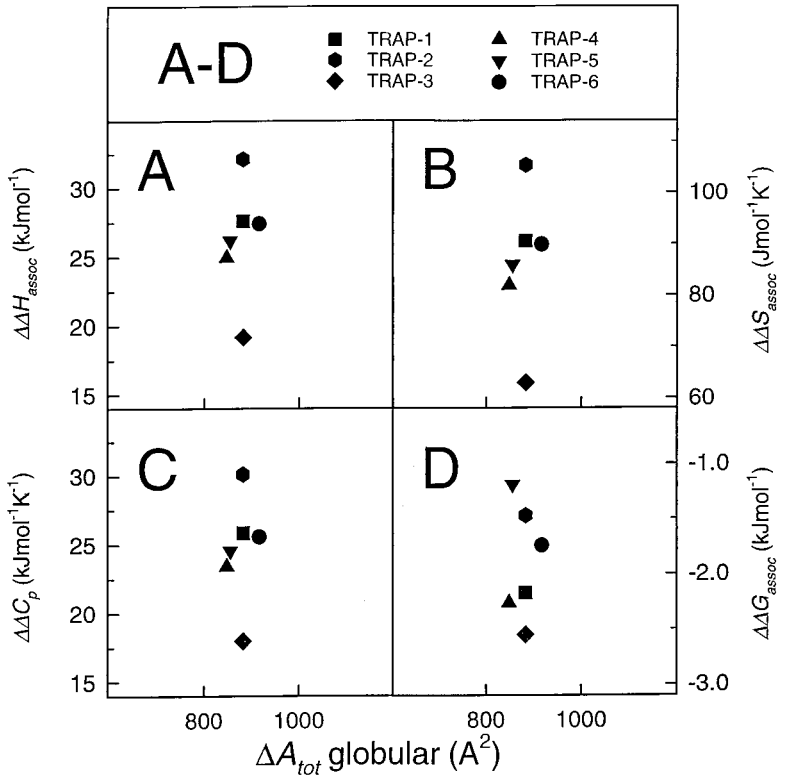

FIGURE 9 Plot of the (*A*) change in enthalpy $\Delta\Delta H^0_{\text{assoc}}$ versus ΔA_{total}; (*B*) change in entropy $\Delta\Delta S^0_{\text{assoc}}$ versus ΔA_{total}; (*C*) change in heat capacity $\Delta\Delta C^0_{\text{p}}$ versus ΔA_{total}; and (*D*) change in Gibbs free energy $\Delta\Delta G^0_{\text{assoc}}$ versus ΔA_{total} for the TRAP-1 and its Alanine-scan peptide analogs at $\varphi = 0.14$.

analogs as depicted in Fig. 7 *C* with respect to temperature, the incremental changes in ΔC^0_{p} with regard to temperature or residue number, namely $\Delta\Delta C^0_{\text{p,T}}$ and $\Delta\Delta C^0_{\text{p,N}_{\text{res}}}$, over the temperature range of 278–338 K are highly diagnostic. Thus, the larger the $\Delta\Delta C^0_{\text{p,T}}$ value, the more sensitive is the peptide to heat, which translates into less structural rigidity of the peptide as it interacts with the nonpolar ligand. The observed variations in the ΔC^0_{p} and $\Delta\Delta C^0_{\text{p}}$ values follow the order expected for the reduction in hydrophobic stabilization of the various TRAP peptides as their structures are kinetically destabilized at higher temperatures. Thus, in a solvent composition whereby $\varphi = 0.14$, the $\Delta\Delta C^0_{\text{p,T}}$ value for the more open TRAP-3 was the lowest at 2.1 $\text{Jmol}^{-1}\text{K}^{-2}$ with the more compact TRAP-4 exhibiting a $\Delta\Delta C^0_{\text{p,T}}$ value of 2.7 $\text{Jmol}^{-1}\text{K}^{-2}$, whereas, for the most compact structure, TRAP-2, the $\Delta\Delta C^0_{\text{p,T}}$ value was 3.5 $\text{Jmol}^{-1}\text{K}^{-2}$. It is well known that polypeptide or protein denaturation or the transfer of nonpolar compounds to more aqueous environments is accompanied by a heat capacity increase and associated enthalpy change (Makhatadze and Privalov, 1990; Graziano et al., 1998). Changes in the partial molar heat capacity of small peptides, such as Gly-Xaa-Gly, in aqueous solutions over a temperature range of 353 K, as determined by differential scanning microcalorimetry, have been reported to be ~0.2–0.3 $\text{kJmol}^{-1}\text{K}^{-1}$ (Hackel et al., 1998, 1999) with corresponding changes in the enthalpy of −10 to −20 kJmol^{-1}. As apparent from Figs. 6 and 7, variations in the ΔC^0_{p} or $\Delta H^0_{\text{assoc}}$ values for all of the TRAP peptides in association with the *n*-octyl ligands have similar magnitudes as the temperature was increased.

In Fig. 9 *C* are shown the plots of $\Delta\Delta C^0_{\text{p}}$ versus ΔA_{total} for the TRAP-related peptides in their folded (globular) conformations (Table 2) over a defined temperature range of 273–338 K and $\varphi = 0.14$, where the trend was apparent for larger $\Delta\Delta C^0_{\text{p}}$ values to follow an increase in the molecular surface-area properties of these peptides. These data reveal two notable effects. First, for TRAP-2, which has the highest $\Delta\Delta C^0_{\text{p}}$ value, it can be concluded that this is the most heat-sensitive TRAP peptide, although TRAP-2 is not the most compact analog, as assessed from the molecular modeling and energy minimization data (see Fig. 3 *C*). A possible explanation for the larger $\Delta\Delta C^0_{\text{p}}$ value of TRAP-2 is that the stabilizing effect of the π–*n* interaction of the Phe^2 with Pro^7 is missing. The change in the thermodynamic properties of TRAP-2 with the Phe^2 replaced by Ala mirrors the effect of elimination of the β-phenyl side-chain group in biological assays, which is associated with the complete loss of receptor activation (Nose et al., 1998a), i.e., TRAP-2 acts as an antagonist.

The other effect evident from the experimental data related to the change in heat capacity versus the molecular surface area is associated with TRAP-3. This TRAP analog was the least heat sensitive of the TRAP-related peptides with the data consistent with the conclusion that TRAP-3 is the least compact peptide. When compared with TRAP-4, which has identical amino acid composition but different

sequence with respect to position 4, the results are in good agreement with the findings from the molecular modeling studies, whereby TRAP-3 has a more open structure with Leu^4 and Pro^7 in a distal position (see Fig. 3 *B*). Analogous behavior was evident for TRAP-3 in the corresponding plots of ΔH^0_{assoc}, ΔS^0_{assoc}, and ΔG^0_{assoc} versus ΔA_{total}, (Fig. 9, *A*, *B*, and *D*).

Several conclusions can be drawn from these results. First, the capacity factor data for the alanine scan TRAP peptide are in good agreement with solvophobic theory (Haidacher et al., 1996; Hearn and Zhao, 1999) for peptides with identical compositions but with different amino-acid sequences. Thus, the thermodynamic discrimination of these TRAP-related peptides is associated with a compensation phenomenon involving rearrangement of water molecules. The observation that TRAP-2 has the highest $\Delta\Delta C^0_p$ value for the binding to immobilized *n*-octyl ligands and thermodynamically is located in a different region of the enthalpy–entropy compensation plot from the other TRAP-related peptides with agonist function is indicative of a different solvent displacement process on interaction with the immobilized nonpolar ligands. This conclusion is also consistent with previous studies with G-protein-coupled receptors and ligand-gated ion channel receptors, indicating that solvent effects might similarly be responsible for the in vitro thermodynamic discrimination of agonists and antagonists. According to currently accepted general models for such association processes involving agonist interaction with β-adrenergic (Weiland et al., 1979) and A_1 adenosine (Borea et al., 1992) receptors, the entropy-driven docking of agonists to the relevant receptor involves displacement of water molecules from a binding site pocket, which previously was filled with a network of structured water molecules. This displacement of structured water from the "receptor" binding site accounts for the observed larger increase in entropy for agonists. A parallel situation appears to occur for the binding of the TRAP-related peptides to the immobilized *n*-octyl ligands, i.e., the differences noted in the interaction thermodynamics of the various TRAP peptide analogs with the nonpolar ligands are qualitatively associated with solvational/desolvational transitions involving equilibrium between closely packed and more open forms of water (Klotz, 1999). Because the magnitude of this phenomenon will be dependent on the molecular characteristics of the peptide, determination of the change in heat capacity $\Delta\Delta C^0_p$ represents a valuable diagnostic parameter, allowing comparative assessment of peptide analogs in respect of their ligand-binding behavior. Second, the derived thermodynamic data are in full agreement with the biophysical and molecular properties of the peptides, allowing the peptide–ligand interaction to be structurally rationalized in conjunction with other experimental procedures, e.g., molecular modeling methods. Third, the above results indicate that synthetic TRAP analogs can be designed to maximize their $\Delta\Delta C^0_p$ values on binding to immobilized nonpolar ligands or the corresponding in vitro receptor systems based on their position in the corresponding entropy–enthalpy plots. Analogs involving intramolecular hydrophobic π–π interaction, in which the stabilizing effect of the interaction between the side chains of Phe^2 and Pro^7 is mimicked, potentially represent one such group of agonist candidates. The combinatorial synthesis and selection of such analogs are currently underway, and their evaluation will be reported subsequently.

These investigations were supported by the Australian Research Council.

REFERENCES

Allinger, N. L. 1977. Conformational analysis 130. MM2. A hydrocarbon force field utilizing V1 and V2 torsional terms. *J. Am. Chem. Soc.* 99:8127–8134.

Allinger, N. L., R. A. Kok, and M. R. Imam. 1988. Hydrogen bonding in MM2. *J. Comp. Chem.* 9:591–595.

Beyermann, M., K. Fechner, J. Furkert, E. Krause, and M. Bienert. 1996. A single-point slight alteration set as a tool for structure-activity relationship studies of ovine corticotropin releasing factor. *J. Med. Chem.* 39:3324–3330.

Borea, P. A., A. Dalpiaz, K. Varani, P. Gilli, and G. Gilli. 2000. Can thermodynamic measurements of receptor binding yield information on drug affinity and efficacy? *Biochem. Pharmacol.* 60:1549–1556.

Borea, P. A., K. Varani, L. Guerra, P. Gilli, and G. Gilli. 1992. Binding thermodynamics of A_1 adenosine receptor ligands. *Mol. Neuropharmacol.* 2:273–281.

Bornstein, P., and G. Balian. 1977. Cleavage at Asn-Gly bonds with hydroxylamine. *Methods Enzymol.* 47:132–145.

Boysen, R. I., and M. T. W. Hearn. 2000. Direct characterisation by electrospray ionisation mass spectroscopy of mercuro-polypeptide complexes after deprotection of acetamidomethyl groups from protected cysteine residues of synthetic polypeptides. *J. Biochem. Biophys. Methods.* 45:157–168.

Boysen, R. I., A. J. O. Jong, J. A. Wilce, G. F. King, and M. T. W. Hearn. 2001. The role of interfacial hydrophobic residues in the stabilisation of the leucine zipper structures of the transcription factors c-*fos* and c-*jun*. *J. Biol. Chem.* 277:23–31.

Boysen, R. I., Y. Wang, H. H. Keah, and M. T. W. Hearn. 1999. Observations on the origin of the non-linear van't Hoff behaviour of polypeptides in hydrophobic environments. *Biophys. Chem.* 77:79–97.

Ceruso, M. A., D. F. McComsey, G. C. Leo, P. Andrade-Gordon, M. F. Addo, R. M. Scarborough, D. Oksenberg, and B. E. Maryanoff. 1999. Thrombin receptor-activating peptides (TRAPs): investigation of bioactive conformations via structure-activity, spectroscopic, and computational studies. *Bioorganic Med. Chem.* 7:2353–2371.

Dunitz, J. D. 1995. Win some, lose some—enthalpy–entropy compensation in weak intermolecular interactions. *Chem. Biol.* 2:709–712.

Fields, G. B., and R. L. Noble. 1990. Solid phase peptide synthesis utilizing 9-fluorenylmethoxycarbonyl amino acids. *Int. J. Pept. Protein Res.* 35:161–214.

Fontenot, J. D., J. M. Ball, M. A. Miller, C. M. David, and R. C. Montelaro. 1991. A survey of potential problems and quality control in peptide synthesis by the fluorenylmethoxycar-bonyl procedure. *Pept. Res.* 4:19–25.

Graziano, G., F. Catanzano, and G. Baraone. 1998. Prediction of the heat capacity change on thermal denaturation of globular proteins. *Thermochimica Acta.* 321:23–31.

Hackel, M., G. R. Hedwig, and H.-J. Hinz. 1998. The partial molar heat capacity and volume of the peptide backbone group of proteins in aqueous solution. *Biophys. Chem.* 73:163–177.

Hackel, M., H.-J. Hinz, and G. R. Hedwig. 1999. A new set of peptide-based group heat capacities for use in protein stability calculations. *J. Mol. Biol.* 291:197–213.

Haidacher, D., A. Vailaya, and C. Horvath. 1996. Temperature effects in hydrophobic interaction chromatography. *Proc. Natl. Acad. Sci. U.S.A.* 93:2290–2295.

Hearn, M. T. W. 1998. High resolution reversed phase liquid chromatography of polypeptides and proteins. *In* Protein Purification. J. C. Janson and L. Ryden, editors. V.C.H. Press, New York. 239–282.

Hearn, M. T. W. 2000. Physicochemical factors in polypeptide and protein purification and analysis by high-performance liquid chromatographic techniques: current status and future challenges. *In* Handbook of Bioseparation. S. Ahuja, editor. Academic Press, San Diego. 72–235.

Hearn, M. T. W. 2001a. Conformational behaviour of polypeptides and proteins in reversed-phase environments. *In* Theory and Practice of Biochromatography. M. A. Vijayalakshmi, editor. Taylor and Francis Publ., London, U.K. 72–141.

Hearn, M. T. W. 2001b. Purification and characterisation of synthetic peptides by reversed-phase chromatography and other high resolution procedures. *In* Synthesis of Peptides and Peptidomimetics. M. Goodman, A. Felix, L. Moroder, and C. Tonioloand, editors. Houben–Weyl–Thieme Publ., Stuttgart, Germany.

Hearn, M. T. W., R. I. Boysen, Y. Wang, and S. Muraledaram. 1999. Peptide conformational behaviour studied by high and low temperature reversed-phase HPLC. *In* Peptide Science—Present and Future. Y. Shimonishi, editor. Kluwer Academic Publishers, Dordrecht, Boston, London. 240–244.

Hearn, M. T. W., and G. L. Zhao. 1999. Investigations into the thermodynamics of polypeptide interaction with nonpolar ligands. *Anal. Chem.* 71:4874–4885.

Houston, M. E., L. H. Kondejewski, D. N. Karunaratne, M. Gough, S. Fidai, R. S. Hodges, and R. E. W. Hancock. 1998. Influence of preformed alpha-helix and alpha-helix induction on the activity of cationic antimicrobial peptides. *J. Pept. Res.* 52:81–88.

Kahn, M. L., Y. W. Zheng, W. Huang, V. Bigornia, D. W. Zeng, S. Moff, R. V. Farese, C. Tam, and S. R. Coughlin. 1998. A dual thrombin receptor system for platelet activation. *Nature.* 394:690–694.

Kaiser, E., R. L. Colescott, C. D. Bossinger, and P. I. Cook. 1970. Color test for detection of free terminal amino groups in the solid-phase synthesis of peptides. *Analyt. Biochem.* 34:595–598.

Keah, H. H., E. Kecorius, and M. T. W. Hearn. 1998. Direct synthesis and characterisation of multi-dendritic peptides for use as immunogens. *Int. J. Pept. Protein Res.* 51:2–8.

Klotz, I. M. 1999. Parallel change with temperature of water structure and protein behaviour. *J. Phys. Chem.* 103:5910–5916.

Kondejewski, L. H., M. Jelokhani-Niaraki, S. W. Farmer, B. Lix, C. M. Kay, B. D. Sykes, R. E. W. Hancock, and R. S. Hodges. 1999. Dissociation of antimicrobial and hemolytic activities in cyclic peptide diastereomers by systematic alterations in amphipathicity. *J. Biol. Chem.* 274:13181–13192.

Lin, F.-Y., W.-Y. Chen, and M. T. W. Hearn. 2001. Microcalorimetric studies of the interaction mechanisms between peptides and proteins and hydrophobic solid surfaces in hydrophobic interaction chromatography: effects of salts, hydrophobicity of the gel and the structure of the proteins. *Anal. Chem.*, 73:3875–3883.

Makhatadze, G. I., and P. L. Privalov. 1990. Heat capacity of proteins. I. Partial molar heat capacity of individual amino acid residues in aqueous solution: hydration effect. *J. Mol. Biol.* 213:375–384.

Makhatadze, G. I., and P. L. Privalov. 1995. Energetics of protein structure. *Adv. Protein Chem.* 47:307–425.

Mari, B., V. Imbert, N. Belhacene, D. F. Far, J. F. Peyron, J. Pouyssegur, E. Van Obberghen-Schilling, B. Rossi, and P. Auberger. 1994. Thrombin and thrombin receptor agonist peptide induce early events of T cell activation and synergize with TCR cross-linking for CD69 expression and interleukin 2 production. *J. Biol. Chem.* 269:8517–8523.

Melander, W. R., D. Corradini, and C. Horvath. 1984. Salt-mediated retention of proteins in hydrophobic-interaction chromatography. Application of solvophobic theory. *J. Chromatogr.* 317:67–85.

Murphy, K. P. 1999. Predicting binding energetics from structure: looking beyond ΔG degrees. *Med. Res. Rev.* 19:333–339.

Murphy, K. P., and S. J. Gill. 1991. Solid model compounds and the thermodynamics of protein unfolding. *J. Mol. Biol.* 222:699–709.

Nose, T., T. Fujita, M. Nakajima, Y. Inoue, T. Costa, and Y. Shimohigashi. 1998a. Interaction mode of the Phe-Phenyl group of thrombin receptor-tethered ligand SFLLRNP in receptor activation. *J. Biochem.* 124: 354–358.

Nose, T., Y. Satoh, T. Fujita, M. Ohno, M. Nakajima, Y. Inoue, Y. Ogino, T. Costa, and Y. Shimohigashi. 1998b. The role of arginine in thrombin receptor tethered-ligand peptide in intramolecular receptor binding and self-activation. *Bull. Chem. Soc. Jpn.* 71:1661–1665.

Purcell, A. W., G. L. Zhao, M. I. Aguilar, and M. T. W. Hearn. 1999. Comparison between the isocratic and gradient retention behaviour of polypeptides in reversed-phase liquid chromatographic environments. *J. Chromatogr.* 852:43–57.

Ross, P. D., and M. V. Rekharsky. 1996. Thermodynamics of hydrogen bond and hydrophobic interactions in cyclodextrin complexes. *Biophys. J.* 71:2144–2154.

Seiler, S. M., M. Peluso, J. G. Tuttle, K. Pryor, C. Klimas, G. R. Matsueda, and M. S. Bernatowicz. 1996. Thrombin receptor activation by thrombin and receptor-derived peptides in platelet and CHRF-288 cell membranes: receptor-stimulated GTPase and evaluation of agonists and partial agonists. *Mol. Pharmacol.* 49:190–197.

Spassov, V. Z., R. Ladenstein, and A. D. Karshikoff. 1997. Optimization of the electrostatic interactions between ionized groups and peptide dipoles in proteins. *Protein Sci.* 6:1190–1196.

Torrens, F. 2000. Polarization force fields for peptides implemented in ECEPP2 and MM2. *Mol. Simul.* 24:4–6.

Troyer, D., R. Padilla, T. Smith, J. Kreisberg, and W. D. Glass. 1992. Stimulation of the thrombin receptor of human glomerular mesangial cells by Ser-Phe-Leu-Leu-Arg-Asn-Pro-Asn-Asp-Lys-Tyr-Glu-Pro-Phe peptide. *J. Biol. Chem.* 267:20126–20131.

Vailaya, A., and C. Horvath. 1996. Retention thermodynamics in hydrophobic interaction chromatography. *Indust. Eng. Chem. Res.* 35: 2964–2981.

Vu, T. K., V. I. Wheaton, D. T. Hung, I. Charo, and S. R. Coughlin. 1991. Domains specifying thrombin–receptor interaction. *Nature.* 353: 674–677.

Weiland, G. A., K. P. Minneman, and P. B. Molinoff. 1979. Fundamental difference between the molecular interactions of agonists and antagonists with the beta-adrenergic receptor. *Nature.* 281:114–117.

Wilce, M. C. J., M. I. Aguilar, and M. T. W. Hearn. 1995. Physicochemical basis of amino acid hydrophobicity scales—evaluation of four new scales of amino acid hydrophobicity coefficients derived from RP-HPLC of peptides. *Anal. Chem.* 67:1210–1219.